

Influence of an ellipsoid on the angular order in a two-dimensional clusterK. Nelissen,^{1,2,*} B. Partoens,¹ and F. M. Peeters^{1,2,†}¹*Departement Fysica, Universiteit Antwerpen, Groenenborgerlaan 171, B-2020 Antwerpen, Belgium*²*Departamento de Física, Universidade Federal do Ceará, Caixa Postal 6030, Campus do Pici, 60455-760 Fortaleza, Ceará, Brazil*

(Received 6 October 2010; revised manuscript received 4 May 2011; published 19 September 2011)

The influence of an ellipsoid on the angular order of two-dimensional classical clusters is investigated through Brownian dynamics simulations. We found the following: (1) The presence of an ellipsoid does not influence the start of the angular melting, but reduces the rate at which the inner rings can rotate with respect to each other. (2) Even a small eccentricity of the ellipsoid leads to a stabilization of the angular order of the system. (3) Depending on the position of the ellipsoid in the cluster, a reentrant behavior in the angular order is observed before full radial melting of the cluster sets in. (4) The ellipsoid can lead to a two-step angular melting process: First, the rotation of the inner rings with respect to each other is hindered by the ellipsoid, but on further increasing the kinetic energy of the system, the ellipsoid just starts to behave as a spherical particle with different mobility. The effect of an ellipsoid on the molten system does not depend crucially on the interparticle interaction, but a softer parabolic confinement reduces the angular stabilization.

DOI: [10.1103/PhysRevE.84.031405](https://doi.org/10.1103/PhysRevE.84.031405)

PACS number(s): 82.70.Dd, 36.40.Sx, 52.27.Lw

I. INTRODUCTION

Melting and crystallization are fundamental processes in nature and have been widely studied. Self-assembly of confined low dimensional field-responsive systems, i.e., pointlike particles, has attracted strong interest in recent years. Part of the interest arises from the fact that it is an ideal model system to understand a variety of phenomena such as crystallization and melting in condensed matter physics and the effect of finite size on it. Examples are systems of charged particles such as colloids [1,2] and dusty plasmas [3,4], which display similar phase behavior as atoms and molecules with the added advantage that the larger size and their slower dynamics make them accessible for real space imaging [5]. Moreover, they have practical applications in the fabrication of new materials, such as special nanoscale magnetic dot arrays [6,7], which are potential materials for high density magnetic data storage devices, field response fabrics [8], and DNA separation devices [9]. Accordingly, numerous experiments investigated a wide variety of such systems, e.g., one-dimensional (1D) and two-dimensional (2D) strongly coupled dusty plasmas [10], colloidal systems restricted in a circular hard wall [11], colloidal system of paramagnetic colloids confined in a parabolic well [12], or hard disks at the liquid-air interface [13]. Many numerical studies have been performed to investigate the crystallization and melting in the above systems by simulating a model system of charged classical pointlike particles, i.e. a Wigner-type crystal [14–25].

The random motion of microscopic particles suspended in a fluid (colloids) is described by Brownian motion. Because the direct detection of translational Brownian motion is relatively easy, many experiments focused on translational diffusion. Consequently, in all numerical studies up to now, rotationally invariant (disklike) particles were considered. The direct visualization of rotational Brownian motion of an ellipsoid (i.e., a prolate spheroid) was only carried out recently [26].

They showed that particle anisotropy leads to dissipative coupling of translation and rotation degrees of freedom as first explored by Perrin [27]. A uniaxial anisotropic particle is characterized by two translational hydrodynamic friction coefficients γ_a and γ_b parallel and perpendicular to the long axis, respectively, with diffusion constants $D_a = k_B T / \gamma_a$ and $D_b = k_B T / \gamma_b$, where k_B is the Boltzmann constant and T the temperature. In general, γ_a is less than γ_b (7), and, consequently, D_a is larger than D_b . The rotational diffusion is defined by a rotational diffusion constant D_θ .

In this paper, the influence of such a single ellipsoid shaped particle on the angular order of two-dimensional classical clusters consisting of spherical particles is investigated. Note that the influence of such an ellipsoidal particle on the diffusive motion of all spherical particles in the cluster will differ fundamentally from the influence of a single spherical particle with just a reduced mobility. In the latter case, the angular motion of the ring that the particle with reduced mobility belongs to is hindered. The effect of the ellipsoid, however, will depend on its orientation, and the orientation of its main axis may be directed along the ring that the particle belongs to or is perpendicular to it, depending on the temperature and the motion of the other particles in the cluster. For a 2D classical cluster with only spherical particles, it was previously found that the particles are arranged in shells, and that melting of finite clusters occurs in two steps [14]. With increasing temperature, intershell motion develops and the system loses angular order. Consecutively, radial diffusion switches on and destroys the shell structure of the cluster. Furthermore, in Ref. [11], a reentrant melting in two-dimensional colloidal clusters was observed: with decreasing the interaction between the magnetic colloidal particles, the first intershell rotation appeared, which destroyed the angular order of the cluster. Further decreasing the interparticle coupling resulted in an unexpectedly regained angular order, followed by a complete melting with a further reduction of the interaction. Brownian dynamics simulations showed that only clusters with short-range interparticle interaction and confined by a hard wall well exhibit such angular freezing before melting, irrespective

*kwinten.nelissen@ua.ac.be

†francois.peeters@ua.ac.be

of the value of viscosity [18]. In the other cases, either of Coulomb clusters or with parabolic confinement, the system shows the usual [14] two-step melting behavior without any reentrance.

In this paper, we address the following questions: (i) Has a single anisotropic particle, which we will call an ellipsoid, any influence on the angular melting temperature in a 2D cluster consisting of spherical particles? (ii) How does such an ellipsoid influence the reentrant melting behavior?

II. MODEL SYSTEMS

We focus on two representative experimental systems, namely, charged particles in a parabolic potential (as in Refs. [3,4]), and colloidal particles confined within a circular hard wall (as in Refs. [11,28]). The 2D parabolic confinement of a particle is modeled by a parabolic potential $V_p(r) = \frac{1}{2}m^*\omega^2r^2$, where m^* is the effective mass of the particle, ω the confinement frequency, and r the particle distance to the center of the confinement potential. Two particles, located at positions \vec{r}_i and \vec{r}_j , experience a screened Coulomb repulsion as typically found in dusty plasmas (and for charged colloids moving in a liquid environment) given by $V(\vec{r}_i, \vec{r}_j) = (e^2/|\vec{r}_i - \vec{r}_j|) \exp(-\kappa|\vec{r}_i - \vec{r}_j|)$, where e is the particle charge, and $1/\kappa$ the screening length where we took $\kappa = 2/a_0$, with a_0 the average interparticle distance.

For the colloidal particles confined in a 2D circular hard wall, the potential has the form $V_p = 0$ for $r \leq R$ and $V_p = \infty$ for $r > R$, where R is the radius of the vessel and r the particle distance to the center of the vessel. The colloids under consideration have a macroscopic magnetic moment in the presence of an external magnetic field, which is directed perpendicular to the 2D plane where the particles are moving in. The resulting repulsive magnetic dipole interaction between the colloidal particles is given by $V(\vec{r}_i, \vec{r}_j) = q_i q_j / |\vec{r}_i - \vec{r}_j|^3$, where $q_i = M_i \sqrt{m_0/4\pi}$ is the ‘‘charge,’’ \vec{r}_i the coordinate of the i th particle, and m_0 the magnetic permittivity. The insets of Fig. 1 show typical configurations of such a colloidal crystal of spherical particles and an ellipsoid at one of the shells.

The characteristic energy of the interparticle interaction for the screened Coulomb cluster is defined as $E_0 = e^2 \exp(-\kappa a_0)/a_0$ and $E_0 = q^2/a_0^3$ for dipole clusters, where $a_0 = [e^2/(\epsilon m \omega_0^2)]^{1/3}$ for parabolic confinement and $a_0 = 2R/\sqrt{N}$ for the hard wall, with N the total number of particles. The coupling parameter is given by $\Gamma = E_0/k_B T$.

In both examples, the ratio of the particle velocity relaxation time versus the particle position relaxation time is very small due to the high viscosity of the medium. Consequently, the motion of the particles is diffusive and overdamped.

Following Ref. [18], which obtained very good qualitative agreement with Ref. [11] in the case of spherical colloidal particles, we neglect the effect of hydrodynamic interactions for spheroids, and following Ref. [29], write the following stochastic Langevin equations of motion for the position of the particles:

$$\frac{d\vec{r}_i}{dt} = \frac{D}{k_B T} \left\{ \frac{dV_{\text{tot}}}{d\vec{r}} + \frac{\vec{F}_L^i}{m_i} \right\}, \quad (1)$$

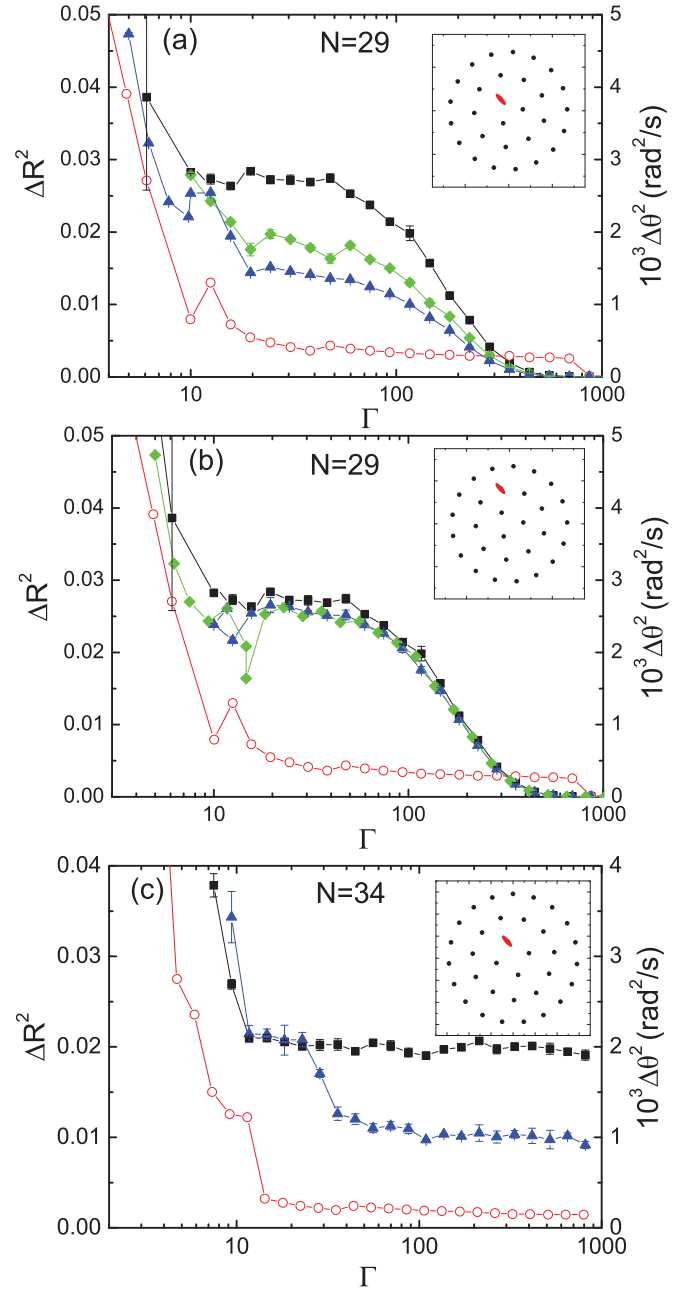


FIG. 1. (Color online) (a) System containing $N = 29$ dipole particles in a circular cavity forming a close-packed configuration with the ellipsoid placed at the inner ring (see inset). (Right scale) The angular diffusion coefficient $\Delta\theta^2$ as a function of the coupling parameter Γ for aspect ratios of the ellipsoid $\phi = 1$ (black squares), $\phi = 5$ (green diamonds), and $\phi = 10$ (blue triangles). (Left scale) ΔR^2 of the spheroids at the middle ring (red circles) for a system with aspect ratio $\phi = 1$ as function of the coupling parameter Γ . (b) Same as (a), but with the ellipsoid placed at the middle ring. The green diamonds show the angular diffusion coefficient of the system for fix particle angle of the ellipsoid. (c) Same as (a), but with $N = 34$ in a non-close-packed configuration

where $V_{\text{tot}}(\vec{r}_i) = \sum_{j=1}^N V(\vec{r}_i, \vec{r}_j) + V_p(\vec{r}_i)$, D is the self-diffusion coefficient of an isolated spherical particle, m_i is the particle mass of the i th particle, N is the total number

of particles (i.e., the spherical ones plus the ellipsoid), and \vec{F}_L^i is a randomly fluctuating force acting on the i th particle due to the surrounding media with variance, given by the fluctuation-dissipation theorem of $\langle 2D \rangle$.

For the motion of the ellipsoid, we assume that the distance between the bottom of the cavity and the particles is large with respect to the particle size. When an ellipsoid with semiaxes (a, b, b) moves along one of its principal axes with velocity v through a fluid with viscosity ν at low Reynolds number, the translational and rotational drag coefficient can be estimated as well:

$$\begin{aligned}\gamma_a &= 6\pi\nu b G_a, \\ \gamma_b &= 6\pi\nu b G_b, \\ \gamma_\theta &= 6\nu V G_\theta,\end{aligned}\quad (2)$$

where G_a , G_b , and G_θ are the geometric factors that characterize the particle anisotropy and V is the volume of the ellipsoid [30]. The geometric factors for prolate ellipsoid diffusion in 3D are analytically given by Perrin's equations [31,32]

$$\begin{aligned}G_a &= \frac{8}{3} \frac{1}{\left[\frac{2\phi}{1-\phi^2} + \frac{2\phi^2-1}{(\phi^2-1)^{3/2}} \ln \left(\frac{\phi+\sqrt{\phi^2-1}}{\phi-\sqrt{\phi^2-1}} \right) \right]}, \\ G_b &= \frac{8}{3} \frac{1}{\left[\frac{\phi}{\phi^2-1} + \frac{2\phi^2-3}{(\phi^2-1)^{3/2}} \ln(\phi + \sqrt{\phi^2-1}) \right]},\end{aligned}\quad (3)$$

and [27,33]

$$G_\theta = \frac{2}{3} \frac{\phi^4 - 1}{\phi \left[\frac{2\phi^2-1}{\sqrt{\phi^2-1}} \ln(\phi + \sqrt{\phi^2-1}) - \phi \right]},\quad (4)$$

with $\phi = a/b$ the aspect ratio. Note that, when $\phi = 1$, the above equations reduce to the translational and rotational Stokes laws.

Further, we will assume that the non-Brownian forces, i.e., the interparticle forces, act on the center of the particles. Following [26,29], we can write the stochastic Langevin equations of motion for the position of the ellipsoid as

$$\begin{aligned}\frac{d\vec{r}}{dt} &= \frac{D_E(\theta)}{k_B T} \left\{ \frac{dV_{\text{tot}}}{d\vec{r}} + \frac{\vec{F}_L}{m_i} \right\}, \\ \frac{d\theta_i}{dt} &= \epsilon_\theta(t),\end{aligned}\quad (5)$$

where $D_E(\theta)$ is a 2×2 matrix with elements $D_E(\theta) = (D_a + D_b)\delta_{ij}/2 + (D_a - D_b)M_{ij}[\theta(t)]/2$ and

$$M_{ij}(\theta) = \begin{pmatrix} \cos 2\theta & \sin 2\theta \\ \sin 2\theta & -\cos 2\theta \end{pmatrix},\quad (6)$$

where \vec{F}_L is a randomly fluctuating force acting on the ellipsoid due to the surrounding media with variance $D_E(\theta)$. $\epsilon_\theta(t)$ represents a random source of noise for angular motion of the particles with variance $2D_\theta$.

The results reported in the next section are obtained from extensive numerical simulations of Eqs. (1) and (5), with a time step $\Delta t \leq 10^{-4}/(nD)$, where $n = N/(\pi R^2)$ is the density of the particles with N the total number of particles and R the radius of the system. The radius of the circular

vessel $R = 36 \mu\text{m}$ and the self-diffusion coefficient of the spheroid $D = 0.35 \mu\text{m}^2/\text{s}$, are taken from the experiment [28]. The diffusion coefficients of the ellipsoid are calculated according to Eqs. (2)–(4) considering the same magnetic content and mass as the spherical particles. In this way, we avoid introducing effects due to a charge difference between the particles (which would also lead to different configurations).

The competition of the circular confinement on the one hand and the interparticle interaction on the other hand leads to the formation of a ringlike structure. All investigated structures in this paper contain three rings, and we placed the ellipsoid on the inner or middle ring. In order to characterize the angular order of the system, we calculate the angular diffusion of the particles over a $30 \text{ min} \times 1000$ time interval. The relative order between the inner and middle ring can be quantified by

$$\Delta\theta^2 = \{ \langle \Delta\theta(t)^2 \rangle - \langle \Delta\theta(t) \rangle^2 \} / t, \quad (7)$$

where $\langle \dots \rangle$ refers to a time averaging, and the mean relative angular displacement rotation of the first shell $\theta_1(t)$ relative to the second $\theta_2(t)$ one is defined as $\Delta\theta(t) = \theta_2(t) - \theta_1(t)$, where $\theta_1(t)$ and $\theta_2(t)$ are defined as the average angular displacement of the particles at the first and second rings, respectively, at time t . $\Delta\theta^2$ is a measure for the rate at which the two rings rotate with respect to each other, and is thus a measure for the angular order in the system. Note that this expression is not the squared one of $\Delta\theta$.

The mean squared radial diffusion (MSRD) coefficient is

$$\Delta R^2 = \frac{1}{N} \sum_{i=1}^N [\langle r_i(t)^2 \rangle - \langle r_i(t) \rangle^2] / a_0^2, \quad (8)$$

which is a measure of the radial order in the system. Further, in this paper, we will consider the MSRD of the middle ring, i.e., we take N in this expression as the number of particles on the middle ring.

III. RESULTS

As mentioned before, we will consider in our simulations systems consisting of spherical particles together with one ellipsoid confined in a circular cavity or a parabolic trap. The competition of a circular confinement on the one hand and the interparticle interaction on the other hand leads to the formation of a ringlike structure. In Refs. [11,34], the melting and reentrant freezing of 2D spherical colloidal particles in confined geometry was studied experimentally and theoretically, respectively. In this paper, the angular stability of this ringlike structure is investigated as function of the aspect ratio of the ellipsoid.

Before starting the Brownian dynamics simulations, we find the zero temperature ground-state configuration, using the Monte Carlo technique as in Ref. [34] and the obtained configuration is used as the starting configuration for the Brownian dynamics simulations.

Following Ref. [18], we consider first dipole clusters in a circular hard wall cavity consisting of $N = 29$ and 34 particles, which have a different type of packing. The ground-state configuration for $N = 29$ is found to be (3:9:17) a close-packed triangular structure while with $N = 34$ (4:11:19)

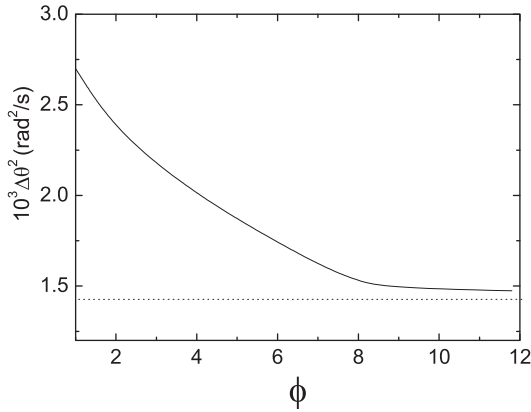


FIG. 2. The angular diffusion coefficient $\Delta\theta^2$ of a dipole cluster for the $\Gamma = 30$ as a function of the aspect ratio ϕ of the ellipsoid for a system containing $N = 29$ dipole particles in a circular cavity forming a close-packed configuration with the ellipsoid placed at the inner ring. The horizontal dotted line shows the limiting case that ϕ goes to infinity.

a non-close-packed structure. Now, we proceed by replacing one of the spheroids of the inner shell by an ellipsoid and start the Brownian dynamics simulations. This approach is justified since the shape of the particle does not influence the ground-state energy and configuration.

Figure 1(a) shows $\Delta\theta^2$ (right scale) for the close-packed system consisting of 28 spherical particles and one ellipsoid on the inner ring for different aspect ratios of the ellipsoid: $\phi = 1$ (i.e., all spherical particles, black squares), 5 (green diamonds), and 10 (blue triangles). One can clearly see that the onset of the angular melting around $\Gamma = 300$ is unchanged in the presence of the ellipsoid. However, the value of $\Delta\theta^2$, which is a measure of the angular order in the system, is strongly reduced by a factor of about 2 for $\phi = 5$. The dependence of the aspect ratio on the angular stabilization is shown in Fig. 2, which gives the value of $\Delta\theta^2$ at $\Gamma = 30$ as function of the aspect ratio ϕ . This figure shows a fast decaying relation between the eccentricity of the ellipsoid and $\Delta\theta^2$. Note that even a small anisotropy in particle shape has immediately an influence on the angular order. For example, an eccentricity of $\phi = 2$ leads to a reduction of the angular diffusion coefficient by 10%. This curve decays to the limiting case, where the ellipsoid is pinned at its initial position, given by the dotted line in Fig. 2. Figure 1(a) shows only the MSRD for the case of $\phi = 1$, as the results for ϕ different from 1 are very similar. The radial melting starts around $\Gamma = 10$.

If we place the ellipsoid at the middle ring of the $N = 29$ system, however, the enhancement of the angular order is much less pronounced, as can be seen in Fig. 1(b). This can be explained by the fact that the inner ring consists of only three particles while the middle ring contains nine particles. The larger the number of particles in a ring, the less the influence of the ellipsoid in that ring has on the angular order of the system.

In Fig. 1(a), a small reentrant melting behavior can be observed between $\Gamma = 10$ and 30. (A reentrant behavior is a behavior where a physical quantity increases first, subsequently decreases, and then increases again as a function of a tuning parameter, here Γ .) However, a strongly enhanced

reentrant behavior in the angular order is observed when the ellipsoid is put on the middle ring, as can be seen from the dip around $\Gamma = 10$ in Fig. 1(b). This is a consequence of the fact that the configuration changes around $\Gamma = 10$. Around this point, the ellipsoid jumps from the middle ring to the inner ring, which immediately reduces $\Delta\theta^2$ to its value of Fig. 1(a). Once the ellipsoid is in the inner ring, it does not return to the middle ring anymore. The reason is that the ellipsoid exhibits slower dynamics than the spherical particles, and it is energetically more favorable to sit in a region with lower particle density, which is at the inner ring. If the spherical particles have enough kinetic energy to cross the potential barrier imposed by the ellipsoid, the neighbor spherical particles push the ellipsoid to the center where there is a lower particle density. This behavior is further enhanced if one fixes the angle of the ellipsoid, with the long axis in the direction of the center of the confinement (which can be realized experimentally by applying an external field). The ellipsoid is then stimulated to go to the center of the confinement because it moves much faster in the direction of the center of the confinement than in the azimuthal direction. This is expressed by the big dip in $\Delta\theta^2$ shown around $\Gamma = 10$ in the curve with green diamonds in Fig. 1(b). The lowest point of this dip corresponds with the angular diffusion curve with blue triangles in Fig. 1(a) at $\Gamma = 10$ and $\phi = 10$.

Let us now look at a non-close-packed system with $N = 34$ particles. From the black squares in Fig. 1(c), for $\phi = 1$ one can see that, even for very large Γ values, there is no angular order between the inner and middle rings. Note that, also in this case, placing an ellipsoid (with $\phi = 5$) reduces the value of $\Delta\theta^2$ significantly [see blue triangles in Fig. 1(c)]. Furthermore, the presence of an ellipsoid results in a two-step angular melting process. Around $\Gamma = 30$, $\Delta\theta^2$ reaches the same value of the spherical particle system when Γ is further reduced. From this point on, the ellipsoid behaves like a spherical particle, although with a different mobility as the spherical particles, because it is not able to hinder the angular motion of the spherical particles: their kinetic energy is large enough to cross the potential barrier imposed by the ellipsoid. Additionally, the average rotation speed of the ellipsoid becomes much faster than the time scale of rotation of the different rings. Decreasing then Γ below 10 results in a fully angular and radially melted system.

At last, we investigate the effect of the functional form of the confinement potential and the interaction. Therefore, we consider a screened Coulomb cluster in a circular hard wall cavity and compare the results with those of a parabolic dot. First, we choose a system consisting of $N = 30$ particles interacting through a short-range screened Coulomb potential confined by a hard wall with ground-state configuration (3:9:18) [see Fig. 3(a)]. Then, we consider a system of $N = 25$ particles interacting through a short-range screened Coulomb potential in a parabolic dot with ground-state configuration (3:9:13) [see Fig. 3(b)]. The number of particles were chosen such that they have the same number of particles on the first two rings. We put in both systems the ellipsoid in the inner ring.

We can see from Fig. 3 that the influence of an ellipsoid on the system for a screened Coulomb interaction but still with a hard wall confinement is similar as for a system with a dipole interaction: the onset of the angular melting is unchanged,

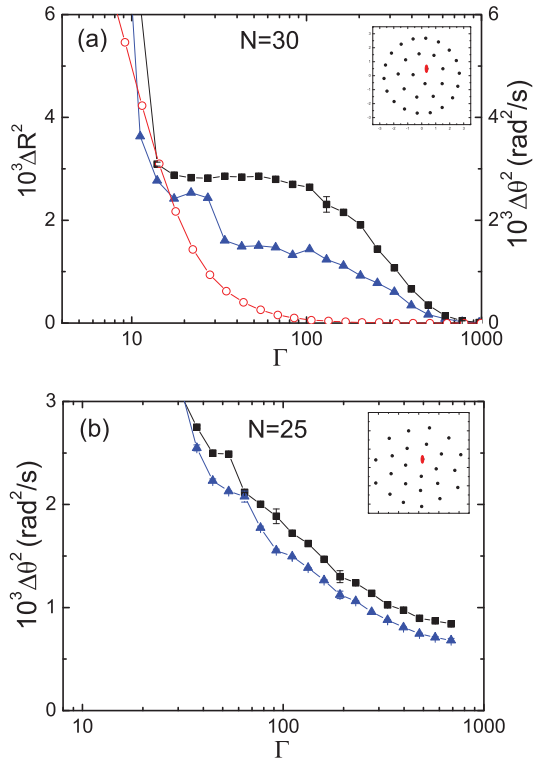


FIG. 3. (Color online) System containing $N = 30$ and 25 screened Coulomb particles with the ellipsoid placed at the inner ring in a (a) circular cavity or (b) parabolic well, respectively. The angular diffusion coefficient $\Delta \theta^2$ of the system as a function of the coupling parameter Γ for aspect ratios of the ellipsoid $\phi = 1$ (black squares) and $\phi = 10$ (blue triangles). ΔR^2 (red circles) of the system as a function of the coupling parameter Γ for aspect ratio of the ellipsoid $\phi = 1$.

however, the angular order is increased. Furthermore, a clear two-step angular melting is observed in Fig. 3(a), as was found for the non-closed-packed system with dipole interparticle interaction. Although there is an enhancement in angular order due to the ellipsoid in the case of a parabolic confinement potential, it is much smaller than for the hard wall case, as can be seen in Fig. 3(b).

IV. CONCLUSIONS

In this paper, we investigated the influence of an ellipsoid on the dynamics of the molten system of 2D classical clusters using Brownian dynamics simulations. We compared the

results for particles interacting through dipole (i.e., long-range interaction) and screened Coulomb (i.e., short-range) interaction confined by a hard wall or parabolic confinement potential. As a representative system, we took the number of confined particles such that we have a three ring structure. We found that, for the system consisting of particles interacting through a dipole potential and confined by a hard wall, which is a good model system for confined magnetic colloids, the presence of an ellipsoid does not influence the start of the angular melting but reduces the rate at which the inner rings can rotate with respect to each other. Even a small eccentricity of the ellipsoid leads to a stabilization of the angular order of the system. The effect of the ellipsoid is most pronounced when it is situated on the inner ring. The ellipsoid was also found to be energetically preferentially situated at this inner ring. Consequently, a reentrant behavior was found in the angular melting when the ellipsoid was placed on the middle ring because of a configurational change: when the kinetic energy of the particles is large enough, they push the ellipsoid to the inner ring, which results in a sudden increase of the angular order. Another effect of the ellipsoid is that it can lead to a two-step angular melting process: First, the rotation of both inner rings with respect to each other is hindered by the ellipsoid, but when further increasing the kinetic energy of the system, the ellipsoid just starts to behave as a spherical particle with different mobility. Further, it was shown that these effects of the ellipsoid on the dynamics of the molten system of 2D classical clusters do not depend crucially on the functional form of the interparticle interaction. However, the angular stabilization of the cluster due to the ellipsoid was found to be less pronounced for particles confined in a parabolic trap.

At present, no experiment has been performed on the investigated system and we hope that our results will be a motivation for experimentalists. A possible experiment would be on a colloidal system consisting of paramagnetic spheroidal colloids in a circular cavity as described in Ref. [11] or a parabolic confined finite size dusty plasma system as in the experiment of Ref. [35] where one changes the eccentricity of one of the spheroids. Our results can serve as a guide on the effect of the anisotropy of particles on the angular and radial order in such 2D clusters.

ACKNOWLEDGMENT

This work was supported by the Flemish Science Foundation (FWO-VI) and CNPq.

[1] P. N. Pusey and W. von Meegen, *Nature (London)* **320**, 340 (1986).
 [2] A. Yethiraj and A. V. Blaaderen, *Nature (London)* **421**, 513 (2003).
 [3] J. H. Chu and Lin I, *Phys. Rev. Lett.* **72**, 4009 (1994).
 [4] H. Thomas, G. E. Morfill, V. Demmel, J. Goree, B. Feuerbacher, and D. Mohlmann, *Phys. Rev. Lett.* **73**, 652 (1994).
 [5] C. A. Murray and R. A. Wenk, *Phys. Rev. Lett.* **62**, 1643 (1989).
 [6] J. Y. Cheng, C. A. Ross, V. Z. H. Chan, E. L. Thomas, R. G. H. Lammertink, and G. J. Vancso, *Adv. Mater.* **13**, 1174 (2001).
 [7] H. C. Kim, X. Q. Jia, C. M. Stafford, D. H. Kim, T. J. McCarthy, M. Tuominen, C. J. Hawker, and T. P. Russell, *Adv. Mater.* **13**, 795 (2001).
 [8] Y. S. Lee, E. Wetzels, and N. Wagner, *J. Mater. Sci.* **38**, 2825 (2003).

- [9] P. S. Doyle, J. Bibette, A. Bancaud, and J.-L. Viovy, *Science* **295**, 2237 (2002).
- [10] B. Liu, K. Avinash, and J. Goree, *Phys. Rev. Lett.* **91**, 255003 (2003).
- [11] R. Bubeck, C. Bechinger, S. Naser, and P. Leiderer, *Phys. Rev. Lett.* **82**, 3364 (1999).
- [12] R. Bubeck, P. Leiderer, and C. Bechinger, *Progr. Colloid. Polym. Sci.* **118**, 79 (2001).
- [13] B. A. Grzybowski, H. A. Stone, and G. M. Whitesides, *Nature (London)* **405**, 1033 (2000).
- [14] V. M. Bedanov and F. M. Peeters, *Phys. Rev. B* **49**, 2667 (1994).
- [15] A. Ghazali and J.-C. S. Levy, *Europhys. Lett.* **74**, 355 (2006).
- [16] K. Nelissen, B. Partoens, and F. M. Peeters, *Phys. Rev. E* **69**, 046605 (2004).
- [17] W. P. Ferreira, F. F. Munarin, K. Nelissen, R. N. Costa Filho, F. M. Peeters, and G. A. Farias, *Phys. Rev. E* **72**, 021406 (2005).
- [18] I. V. Schweigert, V. A. Schweigert, and F. M. Peeters, *Phys. Rev. Lett.* **84**, 4381 (2000).
- [19] K. Nelissen, B. Partoens, I. Schweigert, and F. M. Peeters, *Europhys. Lett.* **74**, 1046 (2006).
- [20] S. Naser, C. Bechinger, P. Leiderer, and T. Palberg, *Phys. Rev. Lett.* **79**, 2348 (1997).
- [21] L. R. E. Cabral, B. J. Baelus, and F. M. Peeters, *Phys. Rev. B* **70**, 144523 (2004).
- [22] K. Nelissen, A. Matulis, B. Partoens, M. Kong, and F. M. Peeters, *Phys. Rev. E* **73**, 016607 (2006).
- [23] K. Nelissen, B. Partoens, and F. M. Peeters, *Europhys. Lett.* **79**, 66001 (2007).
- [24] F. F. Munarin, K. Nelissen, W. P. Ferreira, G. A. Farias, and F. M. Peeters, *Phys. Rev. E* **77**, 031608 (2008).
- [25] K. Nelissen, B. Partoens, and C. Van den Broeck, *Europhys. Lett.* **88**, 30001 (2009).
- [26] Y. Han, A. M. Alsayed, M. Nobili, J. Zhang, T. C. Lubensky, and A. G. Yodh, *Science* **314**, 626 (2006).
- [27] F. Perrin, *J. Phys. Radium* **5**, 497 (1934).
- [28] K. Mangold, J. Birk, P. Leiderer, and C. Bechinger, *Phys. Chem. Chem. Phys.* **6**, 1623 (2004).
- [29] D. L. Ermak and J. A. McCammon, *J. Chem. Phys.* **69**, 1352 (1978).
- [30] M. E. Leunissen, C. G. Christova, A. Hynninen, C. P. Royall, A. I. Campbell, A. Imhof, M. Dijkstra, R. van Roij, and A. van Blaaderen, *Nature (London)* **437**, 235 (2005).
- [31] J. Happel and H. Brenner, *Low Reynolds Number Hydrodynamics* (Kluwer, Dordrecht, 1991).
- [32] Y. Han, A. M. Alsayed, M. Nobili, J. Zhang, T. C. Lubensky, and A. G. Yodh, e-print arXiv:0903.1332v1.
- [33] S. Koenig, *Biopolymers* **14**, 2421 (1975).
- [34] V. A. Schweigert and F. M. Peeters, *Phys. Rev. B* **51**, 7700 (1995).
- [35] A. Melzer, *Phys. Rev. E* **67**, 016411 (2003).